Features of Phyllodes Tumours and Fibroadenomas Differ on MR Images

Midori NOMA[1*)], Kazuo MATSUURA[1)], Masahiro OHARA[1)], Toshiyuki ITAMOTO[1,3)]
Takashi NISHISAKA[2)], Hideki OHDAN[3)]

[1)]*Department of Gastrointestinal, Breast, and Transplantation Surgery Hiroshima Prefectural Hospital*

[2)]*Laboratory for Clinical Investigation Hiroshima Prefectural Hospital*

[3)]*Department of Gastroenterological and Transplant Surgery, Applied Life Sciences, Institute of Biomedical & Health Sciences, Hiroshima University*

Corresponding author: Midori Noma

Mailing address: 1-5-54 Ujina-kanda, Minami-ku, Hiroshima 734-8530, Japan

TEL: +81-82-254-1818; FAX: +81-82-252-6232; E-mail: kimidori@mui.biglobe.ne.jp

Running title: Differentiation of phyllodes tumours and fibroadenomas on MR imaging

Key words: Phyllodes tumour, Fibroadenoma, MRI, Quantitative analysis

ABSTRACT

This retrospective study aimed to determine how the magnetic resonance imaging (MRI) and histopathological findings of phyllodes tumours (PT) and fibroadenomas (FA) correlate and verify whether they are useful for preoperative diagnosis.

We retrospectively reviewed 12 PT and 43 FA that were surgically resected after MRI assessment between 2009 and 2015. The shape and signal intensity (SI) of the tumours on T2-weighted images (T2WI), the apparent diffusion coefficient, and SI were dynamically assessed.

High SI areas suggestive of haemorrhage were significantly more frequent on pre-contrast T1WI of PT than that of FA (66.7% vs. 16.2%, $p = 0.00034$).

The results of the SI analysis showed a higher intratumoural SI for PT than FA on T2WI (7.07 vs. 4.37, $p = 0.0022$).

Overall enhancement was more intense among PT than FA, while SI was significantly higher at 100 seconds (2.03 vs. 1.60, $p = 0.043$) when enhanced effects on pre-enhanced tumours were quantified based on SI ratios.

Not only can MRI morphologically differentiate PT from FA, it can also provide information about tissue composition and vascularization, the quantitation of which seems useful for differentiation.

INTRODUCTION

Phyllodes tumours (PT) are rare fibroepithelial neoplasms that account for 0.3–1.0% of all breast tumours [14]. PT have a leaf-like architecture and infiltrative margins with marked stromal overgrowth and hypercellularity. In contrast to fibroadenomas (FA), which are also fibroepithelial neoplasms, PT can grow very large with a high reported incidence of local relapse [12]. Therefore, wide local excision with margins of at least 1 cm is recommended for all grades of PT [10, 15] since residual PT at excision margins comprise a powerful predictor of local relapse [8, 16]. This is in contrast to treatment for FA, which can be safely managed by simple enucleation, and small FA can be managed non-surgically [5].

Although their management differs in terms of surgical procedures and prognosis, preoperatively differentiating PT from FA is generally considered difficult. Both tumour types feature circumscribed masses, but malignant tumours can be readily ruled out. PT occur in patients aged 35–55 years [13, 15], are usually larger than FA at the time of presentation, and characteristically display sudden size increases [5].

Fine needle aspiration (FNA) can correctly diagnose PT at a rate of 32–77% according to the literature [5]. However, the diagnostic results of core needle biopsy (CNB) have not been summarized, but CNB might be more useful since it can diagnose PT at a rate of 63–86% [4, 17]. However, PT and FA are in fact similarly dimorphic with both epithelial and stromal components. However, although they can be differentiated if stromal hyperplasia is diagnosed, tumour heterogeneity causes problems [6] and sampling issues can interfere with making a definitive preoperative diagnosis.

Mammographic findings show a circumscribed, round, or lobulated mass for both,

rendering differentiation difficult, and both appear as circumscribed hypoechoic masses on ultrasound. However, a cyst identified within a solid lesion on ultrasound is highly suggestive of PT [14, 20]. One study indicated that tissue elastography is useful for diagnosis [1]. High uptake by PT and low uptake in most areas of FA [2, 3] indicate that fluorodeoxyglucose-positron emission tomography (FDG-PET) could help to differentiate these types of tumours. However, the utility of FDG-PET has not been assessed in large-scale studies.

The evaluation of the border region of a mass; presence or absence of septation, cysts and haemorrhage; SI on T2WI; time-intensity curve profiles; and oedema at the tumour margins are reportedly useful for differentiating PT from FA on MRI [5], but the roles of MRI and these features in diagnosis remain obscure. Moreover, classification is often based on visual assessment, and quantitative analysis based on SI or apparent diffusion coefficients (ADC) is rare. Furthermore, a histopathological basis for resected FA specimens is often unavailable.

The present study retrospectively evaluated MR images of PT and FA to determine how they correlate with histopathological findings and verify their applicability to preoperative diagnosis.

MATERIALS AND METHODS

Patients and lesions

We assessed benign FA and PT lesions that were surgically resected from 124 female patients between January 2009 and March 2015. We also retrospectively reviewed the

clinical and imaging findings of 55 lesions from 47 women who underwent preoperative MRI assessment. These patients elected to undergo tumour resection for cosmetic reasons or after physician referral. The institutional review board at Hiroshima Prefectural Hospital approved this study (no. 52, 2015), and all patients provided informed consent prior to participating.

MR imaging

The patients were assessed by MRI using a 3.0 T Magnetom Verio (SIEMENS, München, Germany). Patients were placed in the prone position with dedicated breast coils. An initial scout image was acquired, and then a T2WI (repetition time/echo time, 3400/70 ms; matrix, 448 × 314; slice thickness, 4 mm; gap, 1 mm; field of view, 300 mm) was acquired, followed by a T1-weighted fast-field echo sequence. Subsequently, axial diffusion-weighted images (DWI) were acquired at *b* values of 0, 1000 s/mm^2 (TR/TE, 11900/69; flip angle, 90°; matrix, 128 × 102; slice thickness, 4.0 mm; gap, 1 mm; field of view, 330 mm). Fat suppression was applied using the spectral attenuated inversion recovery technique. ADC maps were automatically generated from the DWI. Three-dimensional dynamic T1-weighted MR images (T1WI) were acquired using a fat-saturated fast low-angle shot sequence (TR/TE, 4.81/1.75; flip angle, 10°; matrix, 480 × 326; slice thickness, 0.9 mm; field of view, 300 mm). Magnevist® contrast medium (Schering-Plough Japan KK., Osaka, Japan) was administered as a bolus injection of 0.1 mmol/kg. Image acquisition was started at 0 and continued at 100, 180, and 300 s thereafter.

Interpretation of MRI findings

Breast MRI findings were interpreted based on three characteristics according to the American College of Radiology Breast Imaging Reporting and Data System (ACR BIRADS) MRI criteria of the tumour mass: shape (lobulated or not), margin (circumscribed or not), and internal enhancement (homogeneous, heterogeneous, or dark internal septation) [11]. Images were evaluated by two breast surgeons with 19 and 16 years of experience in breast MR imaging. All features were determined by consensus. Tumour size; areas of high signal intensity on T1-weighted, non-enhanced fat-saturated images; and cystic changes on T2WI were also analysed.

Intratumoural signal intensity on T2WI and in a dynamic study using contrast medium was assessed. Maximal circular regions of interest (ROI) were placed on T2WI of each tumour and the pectoralis major and SI ratios were calculated. Enhancement profiles that allowed optimal visual enhancement for signal-intensity measurements of kinetics were evaluated using circular ROI. Thereafter, time–signal intensity changes were counted and the parameters for each were calculated (Table 1).

We calculated average ADC by placing ROI on ADC maps corresponding to the ROI for the T2 SI measurements.

Histopathological analysis

All surgical specimens were sliced perpendicular to an arbitrary line. Each slice was then sectioned at 5-mm intervals parallel to a line from the nipple to the lesion and each section was sequentially numbered.

All sections were stained with hematoxylin–eosin and examined by two experienced pathologists to distinguish between FA and PT. PT was classified as benign, intermediate, or malignant.

The authors and a pathologist compared significant MRI findings with histopathological findings. A given MRI section was compared with the approximately corresponding region visualized on a photograph of the gross specimen.

Statistical analysis

Categorical data are presented as absolute and relative frequencies. Differences in continuous variables between the two groups were assessed using the Kruskal-Wallis test, while categorical variables were analysed using Fisher's exact test. P values < 0.05 were considered statistically significant. All data were analysed using SPSS 14.0 J for Windows (SPSS, Chicago, IL, USA).

RESULTS

Clinical background

The histological findings diagnosed 43 and 12 lesions as FA and PT, respectively. Six PT lesions were benign and six were intermediate. Four of the six patients with intermediate PT experienced recurrence.

The patients with FA and PT were aged from 12−49 (median, 34) and 22–58 (median, 42) years, respectively, and the age at FA onset tended to be earlier (Table 2).

Morphology

The median sizes of FA and PT were 3.1 (range, 1.0–9.0) and 4.1 (range, 3.2–10.0) cm, respectively. Thus, PT was significantly larger as described [5].

Areas of high SI were not seen on T2WI, showing liquid components within tumours. Areas of high SI on pre-contrast T1WI suggestive of intratumoural haemorrhage were significantly more frequent among PT (n = 8) than FA (n = 6) (66.7% vs. 16.2%, respectively; p = 0.00034).

All PT were circumscribed, while most were lobulated (83.3%) and heterogeneous (91.7%). The findings of FA were often the same, but other features such as not being circumscribed (18.6%) and internally homogeneous (27.9%) were relatively common (Table 2).

Quantitative analysis with SI and ADC

Signal intensity quantitation is not clearly defined in the Breast Imaging-Reporting and Data System (BI-RADS) classification, and differences in SI are rarely evaluated when for example, tumours exhibit the same degree of high intensity on T2WI. Here we compared the SI of PT and FA on T2WI. Although many reports have compared these tumour types with normal mammary tissue [9], we compared the SI between tumours and pectoralis major tissue as a control to eliminate differences in mammary tissue caused by age. To reflect overall tumour characteristics, each ROI was placed to cover the entire tumour. The results showed that the intratumoural SI on T2WI was higher for PT than FA (7.07 vs. 4.37, respectively; p = 0.0022).

A comparison of ADC when ROI encompassed the entire tumour did not uncover a difference between PT and FA (1.59 vs. 1.58 × 10^{-3} mm^2/sec; Table 2). A comparison of benign and intermediate PT revealed that ADC tended to be lower in the intermediate group, although the difference did not reach statistical significance (data not shown).

We quantified SI on dynamic-enhanced images. The quantitation of enhanced effects

based on SI ratios of pre-enhanced tumours showed greater overall enhancement of PT than FA as well as a significantly higher SI ratio of 100 seconds (%ENH100; 2.03 vs. 1.52, p = 0.043; Table 2).

CNB and FNA findings

Table 3 shows the CNB and FNA results for preoperative diagnosis. CNB was performed in 10 of 12 PT cases, with the results indicating that six of 10 patients had PT, three had FA, and one had intraductal papilloma. The CNB findings of almost all FA cases indicated FA (16 of 18 patients). None of the FNA samples indicated PT.

Histopathological comparisons

High intensity on T2WI and low ADC in images of PT corresponded to stromal hypercellular areas with oedema. High intensity on T1WI corresponded to haemorrhaging (Fig. 1). Areas of high intensity on T2WI and low ADC in images of FA corresponded to epithelial hyperplasia without oedema (Fig. 2).

DISCUSSION

The present study targeted PT and FA surgical patients who underwent preoperative MRI. Tumours that are small or do not exhibit growth tendencies are not resected in actual clinical practice. On the other hand, tumours such as large PT that are indicated for mastectomy are not eligible for MRI as tumour spread is not evaluated. Problems arise in the clinical setting when attempting to differentiate medium-sized PT and FA with growth tendencies. We believe that the preoperative diagnosis of these tumours in

patients who are assessed by MRI is of particular significance in selecting the appropriate surgical procedures.

Although PT are generally thought to develop later in life and be larger than FA [5], the present study found a significant difference in age at onset but not in size. Furthermore, all pathologically diagnosed PT were benign or intermediate in this study. Selection bias might have caused this because only tumours that were difficult to judge as PT or FA were assessed by MRI.

High-intensity signals suggesting haemorrhage on T1 fat-saturated pre-enhanced images were significantly more frequent in PT than FA. Some studies have found that cysts and haemorrhage are typical of PT and that they are apparently associated with regressive changes when PT grow rapidly [5, 7]. Therefore, these changes are often found in large tumours at frequencies that vary among reports. We did not find any hyperintense signal lesions on T2WI indicating cystic changes. This might have been because we analysed relatively small PT, and detecting microcysts within PT exhibiting high-intensity signals on T2WI was difficult. Yabuuchi et al. reported that the morphological evaluation of cyst walls in PT is useful for determining malignancy [19]. However, they evaluated cystic changes on contrast-enhanced subtraction images. That is, they judged high-intensity signals without contrast effects on T1 fat-saturated images of cysts that might have actually intratumoural haemorrhage. We found here that high-intensity signals on T1 fat-saturated pre-enhanced images rather indicated haemorrhage than cysts and that T2WI were more sensitive for identifying medium-sized tumours.

Both PT and FA have circumscribed margins on MRI [5]. All PT in the present study were circumscribed, whereas eight (18.6%) FA were not. This is not typical of benign tumours, but some might have been rendered as non-circumscribed because of poor

enhancement. Wurdinger et al. also found that 24 (29.6%) of 81 FA were not circumscribed [18]. Morphologically, more PT tended to have a heterogeneous centre and septations, but the difference did not reach significance. The fact that these findings, which appear to reflect heterogeneous hyperplasia of PT and are insufficient for a diagnosis, agrees with previous findings [7, 18]. The morphological classification of tumours in BI-RADS version 3 includes a lobulated shape as a variant of an oval shape [11]. However, reports indicate that lobulation is characteristic of PT and might facilitate the differentiation between PT and FA [7].

Various studies investigated SI on T2WI in PT and FA. Kuhl et al. found higher SI in 62–76% of FA than in normal mammary glands and that most PT have high SI but sometimes include low or iso-SI components [9]. Signal intensity is often clinically evaluated by comparison with normal mammary glands. However, considering the difference in age at onset between PT and FA, healthy mammary gland signals might differ. We objectively and quantitatively compared the SI of PT and FA with that of the major pectoralis muscle in the same imaging screen and found that the SI was significantly higher for PT than FA. This likely reflects the stromal cell proliferation and oedema in PT.

The ADC values of breast tumours are inversely correlated with tumour cellularity. Yabuuchi et al. reported that the ADC is decreased in more malignant PT, that is, they are highly cellular [19]. The present study also showed that the ADC tended to be lower in borderline than in benign PT, whereas those in PT and FA did not significantly differ. This is presumably because PT are characterized by stromal cell proliferation, whereas FA have more epithelial components.

In ACR BI-RADS MRI, tumour kinetics are evaluated during the early phase within the

first 2 minutes and the subsequent delay phase, while malignancy is generally determined from curves [11]. However, others found that the kinetic curve is not useful for differentiating PT and FA [18]. We quantitatively compared SI during all phases, rather than with curves, and found a significantly higher SI ratio at 100 sec (%ENH100) in PT than in FA.

Making an accurate evaluation using visual film assessment is difficult. Signal intensity can be easily quantified using current software. Therefore, these findings might support a differential diagnosis of PT and FA.

CNB has become a popular means of diagnosing PT and FA. We found that CNB has 60% sensitivity, 100% specificity, and positive (PPV) and negative (NPV) predictive values of 100% and 81.8%, respectively, for diagnosing PT. Although CNB was not obtained from all tumours because of the low sensitivity, the high PPV suggested that wide resection with a margin should be the treatment of choice when PT is diagnosed.

Diagnosing PT by MRI using a single parameter is difficult. Appropriate SI cut-off values of 4.81 for T2WI and 1.68 for %ENH100 were set using receiver operating characteristics curves since these two parameters significantly differed between PT and FA. The sensitivity for a diagnosis of PT was maximal when values for one or both parameters were high (sensitivity, 100%; specificity, 39.5%; PPV, 31.6%; NPV, 100%). Local resection without a margin could proceed for tumours that are not diagnosed as PT due to a high NPV considering cosmetic considerations.

In conclusion, quantitative MRI findings associated with tissue composition and vascularization in addition to morphological differences appear useful for distinguishing PT from FA.

REFERENCES

1. **Adamietz, B.R., Kahamann, L., Fasching, P.A., Schulz-Wendtland, R., Uder, M., Beckmann M.W., et al.** 2011. Differentiation between phyllodes tumor and fibroadenoma using real-time elastography. Ultraschall Med, **32 Suppl 2**: E75-9.
2. **Baba, S., T. Isoda, Y. Maruoka, Y. Kitamura, M. Sasaki, T. Yoshida, et al.**, 2014. Diagnostic and prognostic value of pretreatment SUV in 18F-FDG/PET in breast cancer: comparison with apparent diffusion coefficient from diffusion-weighted MR imaging. J Nucl Med, **55**(5): 736-42.
3. **Dong, A., Y. Wang, J. Lu, and C. Zuo.**, 2016. Spectrum of the Breast Lesions With Increased 18F-FDG Uptake on PET/CT. Clin Nucl Med, **41**(7): 543-57.
4. **Florentine, B.D., Cobb, C.J., Frankel, K., Greaves, T. and Martin, S.E.,** 1997. Core needle biopsy. A useful adjunct to fine-needle aspiration in select patients with palpable breast lesions. Cancer, **81**(1): 33-9.
5. **Jacklin, R.K., Ridgway, P.F., Ziprin, P., Healy, V., Hadjiminas, D, and A, Darzi.,** 2006. Optimising preoperative diagnosis in phyllodes tumour of the breast. J Clin Pathol, **59**(5): 454-9.
6. **Jara-Lazaro, A.R., Akhilesh, M., Thike, A.A., Lui, P.C., Tse, G.M. and Tan, P.H.,** 2010. Predictors of phyllodes tumours on core biopsy specimens of fibroepithelial neoplasms. Histopathology, **57**(2): 220-32.
7. **Kamitani, T., Matsuo, T., Yabuuchi, H., Fujita, N., Nagao, M., Kawanami, M., et al.**, 2014. Differentiation between benign phyllodes tumors and fibroadenomas of the breast on MR imaging. Eur J Radiol, **83**(8): 1344-9.
8. **Kapiris, I., Nasin, N., A.Hern, R., Healy, V. and Gui, G.P.,** 2001. Outcome and

predictive factors of local recurrence and distant metastases following primary surgical treatment of high-grade malignant phyllodes tumours of the breast. Eur J Surg Oncol, **27**(8): 723-30.

9. **Kuhl, C.K., Klaschik, S., Mielcarek, P., Gieseke, J., Wardelmann, E. and Schil, H.H.,** 1999. Do T2-weighted pulse sequences help with the differential diagnosis of enhancing lesions in dynamic breast MRI? J Magn Reson Imaging, **9**(2): 187-96.
10. **Mangi, A.A., Smith, B.L., Gadd, M.A., Tanabe, K.K., Ott, M.J. and Souba, W.W.,** 1999. Surgical management of phyllodes tumors. Arch Surg, **134**(5): 487-92; discussion 492-3.
11. **Morris, E.A., C.E. Comstock, and C.H. Lee,** 2013. ACR BI-RADS® Atlas 5 Edition.
12. **Parker, S.J. and S.A. Harries**, 2001. Phyllodes tumours. Postgrad Med J, **77**(909): 428-35. **[Please check the journal format.]**
13. **Reinfuss, M., Mitus, J., Duda, K., Stelmach, A., Ry's, J. and Smolak, K.,** 1996. The treatment and prognosis of patients with phyllodes tumor of the breast: an analysis of 170 cases. Cancer, **77**(5): 910-6.
14. **Rowell, M.D., Perry, R.R., Hsiu, J.G. and Barranco, S.C.** 1993. Phyllodes tumors. Am J Surg, **165**(3): 376-9.
15. **Salvadori, B., Cusumano, F., Del, Bo.R., Delledonne, V., Grassi, M., Rovini, D., et al.** 1989. Surgical treatment of phyllodes tumors of the breast. Cancer, **63**(12): 2532-6.
16. **Tan, P.H., Thike, A.A., Tan, W.J., Thu, M.M., Busmanis, I., Li, H., et al.** 2012. Predicting clinical behaviour of breast phyllodes tumours: a nomogram based on histological criteria and surgical margins. J Clin Pathol, **65**(1): 69-76.

17. **Ward, S.T., Jewkes, A.J., Jones, B.G., Chaudhn, S., Hejmadi, R.K., Ismail, T., et al.**, 2012. The sensitivity of needle core biopsy in combination with other investigations for the diagnosis of phyllodes tumours of the breast. Int J Surg.

18. **Wurdinger, S., Herzoq, A.B., Fischer, D.R., Marx, C., Raabe, G., Schneider, A., et al.**, 2005. Differentiation of phyllodes breast tumors from fibroadenomas on MRI. AJR Am J Roentgenol, **185**(5): 1317-21.

19. **Yabuuchi, H., Soeda, H., Matsuo, Y., Okafuji, T., Eguchi, T., Sakai, S., Kuroki, S., et al.**, 2006. Phyllodes tumor of the breast: correlation between MR findings and histologic grade. Radiology, **241**(3): 702-9.

20. **Yilmaz, E., S. Sal. and B. Lebe.,** 2002. Differentiation of phyllodes tumors versus fibroadenomas. Acta Radiol, **43**(1): 34-9.

Table 1: Magnetic resonance imaging parameters

Parameter	Calculation	Definition
SI on T2WI	SItumor/SImuscle	Relative Intratumoral SI to muscle SI on T2-weighted image
%ENH100	(SI100-SIbase)/SIbase	Relative ENH 100 second after CM injection to before CM
%ENH300	(SI300-SIbase)/SIbase	Relative ENH 300 second after CM injection to before CM

CM: Contrast medium, ENH: Enhancement, SI: Signal Intensity

Table 2: Clinical background and MRI findings of phyllodes tumours and fibroadenomas.

Tumor Characteristics	Phillodes tumor (N=12)	Fibroadenoma (N=43)	P value
Age	42.0±10.7	34.0±10.1	0.055
Recurrence	4	0	**0.00096**
Size(cm)	4.1±2.2	3.1±1.8	**0.0038**
Cystic change on T2-weighted image	0	0	-
High signal intensity on T1-weighted image	8	6	**0.00034**
Mass shape; Lobulated	10	17	**0.018**
Margin			
Circumscribed	12	35	0.11
Not circumscribed	0	8	
Internal enhancement characteristics			
Homogeneous	1	12	0.15
Heterogeneous	11	31	
Dark internal septations	3	7	0.79
SI on T2-weighted image	7.07±2.46	4.37±2.61	**0.0022**
ADC (x10^{-3} mm^2/sec)	1.59±0.33	1.58±0.32	0.81
Kinetic pattern			
%ENH100	2.03±0.60	1.52±0.77	**0.043**
%ENH300	2.25±0.61	1.85±0.71	0.075

	Phillodes tumor (N=12)	Fibroadenoma (N=43)
Core needle biopsy	(N=10)	(N=18)
Fibroadenoma	3	16
Phyllodes tumor	6	0
Other	1 (intraductal papilloma)	2 (normal breast tissue)
Fine needle aspiration	(N=2)	(N=15)
Fibroadenoma	2	15
Phyllodes tumor	0	0
Other	0	0

Table 3: Preoperative diagnostic findings of core needle biopsy and fine needle aspiration.

Figure 1: A female patient aged 34 years with a borderline phyllodes tumour

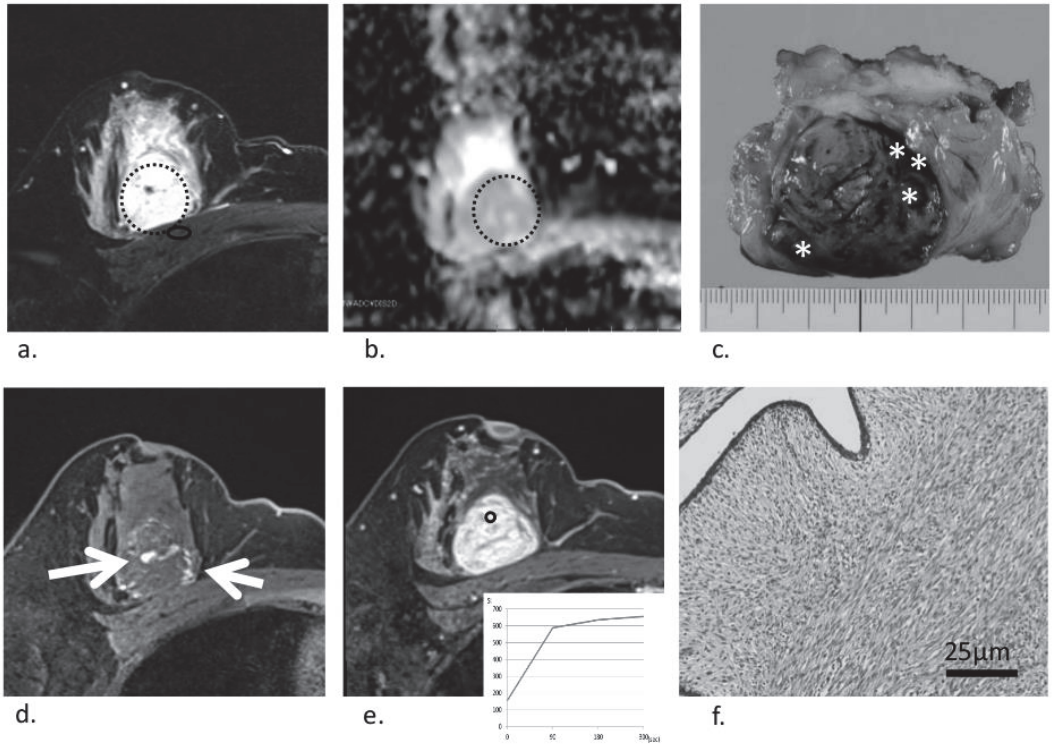

(a) T2-weighted image showing a mass with high signal intensity (SI). The region of interest (ROI; circle) for the SI measurement was placed on the tumour and the pectoralis major muscle.

(b) Apparent diffusion coefficient (ADC) map constructed from diffusion-weighted images with a *b* factor of 0 and 1000 s/mm^2. The circular ROI included the entire tumour; the ADC was 1.47 × 10^{-3} mm^2/s.

(c) Cut surface of a tumour specimen showing haemorrhagic changes (*). The high-SI area in (b) histopathologically corresponds to hypercellular stroma, not a cystic

lesion.

(d) Pre-contrast T1 fat-saturation images showing scattered areas of high SI suggestive of intratumoral and peripheral haemorrhage (arrow).

(e) The tumour is showing strong enhancement at the dynamic early phase (100 s). Circle, ROI of the kinetic analysis placed in the small area of rapid enhancement. Time–signal intensity curve revealing rapid enhancement and a plateau.

(f) Stromal hypercellularity areas with oedema visible on haematoxylin-eosin–stained specimens.

Figure 2: A female patient aged 24 years with fibroadenoma

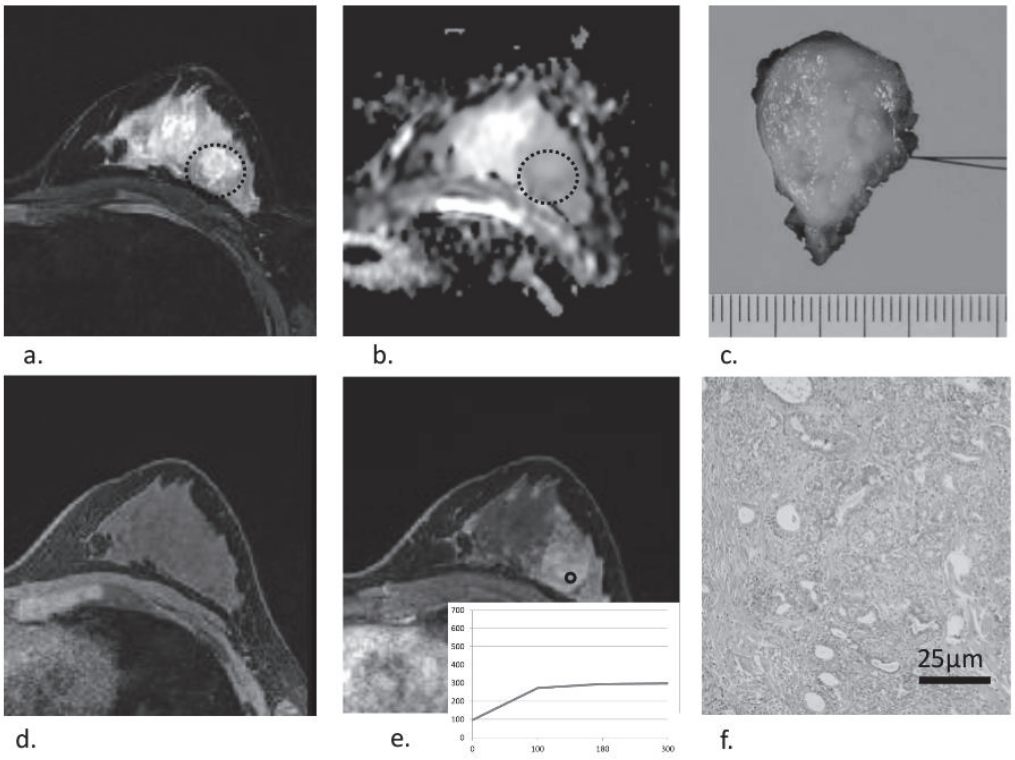

(a) T2-weighted image showing a mass with iso–signal intensity (SI).

(b) The apparent diffusion coefficient was 1.34×10^{-3} mm^2/sec.

(c) Cut surface of the tumour specimen revealing no haemorrhagic change.

(d) Pre-contrast T1 fat-saturation images showing no areas of high SI.

(e) Tumour showing slight enhancement without circumscribed margins in the early phase. Time–signal intensity curve showing persistent pattern.

(f) Epithelial hypercellular areas without oedema on specimens stained with haematoxylin-eosin.